Heliyon 9 (2023) e14710

Contents lists available at ScienceDirect

Heliyon

journal homepage: www.cell.com/heliyon

Research article

Analysis on the genome of a teschovirus type 1 isolates with swine diarrhea

Baotai Zhang [a,e,1], Rongli Guo [a,1], Li Xiao [a,e], Chunyan Zhong [a,g], Xuesong Yuan [a,d], Jin Huang [a,d], Xuejiao Zhu [a,d], Jinzhu Zhou [a], Baochao Fan [a,c,d,f], Tao Xue [b], Chuanmin Liu [a,b,c], Xing Zhu [e,**], Jizong Li [a,b,c,d,f,*], Bin Li [a,c,d,f,***]

[a] Institute of Veterinary Medicine, Jiangsu Academy of Agricultural Sciences, Key Laboratory of Veterinary Biological Engineering and Technology, Ministry of Agriculture, Nanjing, 210014, China
[b] School of Pharmacy, Linyi University, Linyi, 276000, China
[c] Institute of Life Sciences, School of Food and Biological Engineering, Jiangsu University, Zhenjiang, 212013, China
[d] College of Veterinary Medicine, Nanjing Agricultural University, Nanjing, 210095, China
[e] College of Animal Science, Guizhou University, Guiyang, 550025, China
[f] Jiangsu Co-Innovation Center for Prevention and Control of Important Animal Infectious Diseases and Zoonoses, Yangzhou University, Yangzhou, 225009, China
[g] Department of Bioengineering, Qianxinan Vocational and Technical College for Nationalities, Xingyi, 562400, China

ARTICLE INFO

Keywords:
PTVs
High-throughput sequencing
VP1
Diarrhea
Phylogenetic analysis

ABSTRACT

Porcine Teschoviruses (PTVs) are associated with polioencephalomyelitis and various diseases, including reproductive and gastrointestinal disorders of pigs and wild boars, but rarely detected in the feces of pigs. In this study, a sample of swine diarrhea that tested positive for PTVs is subjected to high-throughput sequencing. The viral genome was 7221 nucleotides (nt) in length, which was consisted of twelve genes. Phylogenetic analysis showed and it was closely related to the PTV-HNMY(MG755212.1). The nucleotide homology of VP1 gene of PTVs JS2021 with PTV-1AF 296102.1 reached 82.97%, belonging to a branch of PTV-1 serotype. The nucleotide homology of VP1 protein with other serotypes of PTV is quite different from that of other serotypes of PTV. Bioinformatics analysis showed that PTVs have four capsid proteins, namely VP1, VP2, VP3 and VP4. The VP1 encodes a 29 kDa protein, which is the main protective antigen, a theoretical isoelectric point of 6.73, no transmembrane domain, no signal peptide and potential phosphorylation site. The VP1 protein is an unstable hydrophilic intracellular protein, which contains four secondary structures: irregular curl (c), extended chain (e), α-helix (h) and β-folded (t). The tertiary structure is heart-shaped and has multiple B cell epitopes. By analyzing the tertiary structure, we found that the amino acid at position 129 of VP1 mutated and reduction a larger alpha helix. This may lead to the main cause of piglet diarrhea. These findings enriched our knowledge of the viruses in the role of swine diarrhea, and help to develop an effective strategy for disease prevention and control.

* Corresponding author. Institute of Veterinary Medicine, Jiangsu Academy of Agricultural Sciences, Key Laboratory of Veterinary Diagnosis, Jiangsu Academy of Agricultural Sciences, Key Laboratory of Veterinary Biological Engineering and Technology, Ministry of Agriculture, Nanjing, 210014, China.
** Corresponding author. College of Animal Science, Guizhou University, Guiyang, 550025, China.
*** Corresponding author. Institute of Life Sciences, School of Food and Biological Engineering, Jiangsu University, Zhenjiang, 212013, China.
E-mail addresses: zhuxing72@126.com (X. Zhu), lijizong22@sina.com (J. Li), libinana@126.com (B. Li).
[1] These authors contributed equally to this work.

https://doi.org/10.1016/j.heliyon.2023.e14710
Received 13 October 2022; Received in revised form 8 March 2023; Accepted 15 March 2023
Available online 21 March 2023

1. Introduction

Porcine enteric diseases resulting in diarrhea or intestinal pathology and poor growth performance cause huge economic losses around the world [1,2]. It has been suggested that various etiological agents acting either individually or synergistically including viruses, bacteria, and parasites are responsible for clinical consequences such as diarrhea and poor growth in pigs [3]. Viruses, including picornaviruses such as porcine sapelovirus (PSV), porcine enteroviruses (PEV), and porcine teschoviruses (PTV), have been identified in association with various disorders, including diarrhea, polioencephalomyelitis, respiratory distress, dullness, skin lesions, pyrexia, and flaccid paralysis [4,5]. However, PTVs are rare reported in China that can be detected in piglet diarrhea feces, which has aroused our great interest.

Teschovirus encephalomyelitis, also known as Teschen or Talfan disease, was first reported in Teschen, Czechoslovakia in 1929 [6]. Since then, the disease spreads throughout Europe and other continents during the 1940s and 1950s, causing devastating economic losses [7]. At present, a mild form of the disease, with the exception of an outbreak in 2009 in the Republic of Haiti, has been described in many countries [8]. The first documented PTV isolate (Swine/CH/IMH/03) in China was identified in 2003, and epidemiological studies related to PTV in China have been reported since then [9]. In general, PTVs are non-pathogenic, the infected swine are most often asymptomatic [10]. Sporadic cases have been associated with a variety of clinical symptoms, including polioencephalomyelitis, female reproductive disorders, and enteric and respiratory disease [11], However, there are no other published assays for analysis on the complete genome of Teschovirus with swine diarrhea.

In November 2021, middle to servere diarrhea of unknown pathogen broke out on a swine farm in Jiangsu province, China. The collected samples were negative for PDCoV, PEDV, TGEV, RV, ASFV, and positive for PTVs by RT-PCR. According to high-throughput sequencing, the approximately complete genome sequences were obtained and compared with other known PTV sequences available in GenBank database, moreover, the genome component and protein-coding regions were analyzed further. These findings enriched our knowledge of the viruses in the role of swine diarrhea, and help to develop an effective strategy for disease prevention and control.

2. Materials and methods

2.1. Samples and RT-PCR assays

Three calf diarrhea samples from Jangsu Province, manifesting as weakness, fever, excretion of watery feces, and accompanied by a foul smell, were subjected to RNA extraction using HiPure Total RNA Mini Kit (AnGen, Guangzhou, China). The total RNA was further reverse transcribed into cDNA using a Vazyme Reverse Transcription Kit (Vazyme, Nanjing, China). PCR amplification was performed using 2 × Taq Master Mix (Vazyme, Nanjing, China) with the following primers: For PTVs: VP1 sense, VP15′-CTAAAGGGACCCTC-CAACAT-3′; VP1 antisense, 5′-CTCATCATAGGCTTCACAAA-3′. The above pairs of primers were designed with reference to sequences GenBank accession AJ011380 [12]. PCR reactions were performed with 2 μL of cDNA templates added to 18 μL of reaction mixture, containing final concentrations of 0.5 μM of each primer. The cDNA was amplified by 35 cycles of denaturation at 95 °C for 30 s, annealing at 55 °C for 35 s, and extension at 72 °C at 1 kb/min, and finally extended at 72 °C for 10 min.

2.2. Viral isolation

Feces that were PTV positive by PCR were used for virus isolation. Briefly, a 10% feces homogenate was prepared with minimal essential medium (MEM), followed by three freeze-thaw cycles. All homogenates were subjected to centrifugation at 12,000 rpm for 15 min and filtered through 0.22-μm filters. One ml of filtrate was used to inoculate swine testis (ST) cells that had been grown to 70–80% confluence in 25-cm^2 cell culture flasks. After incubation for 2 h (h), the supernatants were discarded, and the cells were washed three times and incubated for 36–48 h at 37 °C. Then, the culture was freeze-thawed three times at −80 °C for use in the next passage. When the next passage, the obtained virus liquid will be diluted 100 times the ratio of DMEM and inoculated in a single layer of ST cells, cultured in a 5% carbon dioxide thermostatic incubator for 2 h, discard the supernatants, add DMEM medium of 2% fetal bovine serum, and observe the lesion every day.

2.3. Next generation sequencing (NGS)

The extracted total RNA was sent to Shanghai Tanpu Biotechnology Co. Ltd (Shanghai, China). The genome DNA was broken into small fragments of hundreds of bases, and the base was added to the end. After the DNA fragment becomes a single chain, it is fixed on the chip by complementarity with the base on the surface of the chip. After 30 rounds of repeated amplification, each single molecule is amplified 1000 times, becoming a monoclonal DNA cluster. Modified DNA polymerase and dNTP with 4 fluorescent markers are added. Count the results of fluorescent signals collected in each round, resulting in gene amplification and deep sequencing of the virus strain. Subsequent DNase treatment and cleanup was followed by second-strand synthesis before library preparation using Nextera XT reagents and sequencing on the NovaSeq 6000 (Illumina). Read quality trimming was performed using the Skewer, with an additional trimming filter for unreliable sequences after a user-specified quality score. Host read subtraction by read-mapping was performed with the BWASW program against ribosomal RNAs (16, 18, 23, 28, 5S, and internal transcribed spacers rRNA were retrieved from https://www.ncbi.nlm.nih.gov/, accessed on March 15, 2021), bacterial genome sequences, and the latest host organism genome sequences. We then used SPAdes and MEGAHIT software to de novo assemble the reads obtained after removal of the above-mentioned

contamination sequence. The de novo assembly followed the A5-miseq pipeline. The final scaffolds were subjected to bwasw read mapping and a mega blast homology search against the NCBI NT database, were selected for further analyses. Selected sequences were aligned using Clustal-W and phylogenetic trees, created using the maximum likelihood (ML) method with the best fitting model, as determined by MEGA 7. The robustness of different phylogenetic nodes was assessed using 1000 bootstrap replicates for nucleotide sequences.

2.4. Phylogenetic and genome analysis

Fristly, analyze the whole genome structure of PTVs in ORF Finder (https://www.ncbi.nlm.nih.gov/orffinder/) online software.

Next, compare and download the reference sequences in GenBank database of NCBI website, align the nucleotide sequences by Clustal W method in MEGA7.0, construct the phylogenetic tree by neighbor-joining method (NJ), and set the display value to repeat 1000 times.

At the same time, use MegAlign in DNAstar series software to analyze the homology of amino acid sequences encoded by these nucleotides to master the genetic evolution of strains.

The physiological characteristics of VP1 protein are analyzed with relevant software. Fristly, analyze the molecular weight, amino acid composition, isoelectric point and instability coefficient of genomic capsid protein in Prot-Param (https://web.expasy.org/protparam/) online software; Then, using online software ProtScale (https://web.expasy.org/protscale/) to analyze the hydrophilic and hydrophobic properties of genome; SignalP 4.0 Server (http://www.cbs.dtu.dk/services/SignalP-4. 0/) was used to analyze key gene signal peptides; Next, prediction of transmembrane domains of key genes through TMHMM Server (http://www.cbs.dtu.dk/services/TMHMM/) online tool; Prediction of potential amino acid phosphorylation sites at NetPhos3.1 Server (http://www.cbs.dtu.dk/services/NetPhos/); Besides, Using IEDB (http://tools.iedb.org/bcell/) and BCPREDS (http://ailab-projects1.ist.psu.edu:8080/bcpred/predict.html) online software, the B cell linear epitope of genome-encoded protein was predicted; Finally, using SOPMA (https://npsa-prabi.ibcp.fr/cgi-bin/npsa_automat.pl? Page = npsa_sopma.html) and SWISS-MODEL (https://swissmodel.expasy.org/) online websites to predict the secondary and tertiary structures of key proteins.

3. Results

3.1. Viral isolation

The collected samples were negative for PDCoV, PEDV, TGEV, RV, ASFV, and positive for PTVs by RT-PCR. One ml of filtrate was used to inoculate swine testis (ST) cells that had been grown to 70–80% confluence in 25-cm^2 cell culture flasks. After incubation for 2 h (h), the supernatants were discarded, add DMEM culture solution containing 2% fetal bovine serum, cultured in 5% carbon dioxide thermostatic incubator, observe the changes of CPE, and the isolate produced cytopathic effect from the 2nd passage, specificity primers were used to amplify from virus cultures by RT-PCR. Under the ultraviolet lamp, the RT-PCR product of the VP1 gene fragment of PTVs JS2021 has a molecular weight of 957 bp at 1% agar (Fig. 1A and B). These results suggested successful viral isolation and amplication, the virus was named PTVs JS2021.

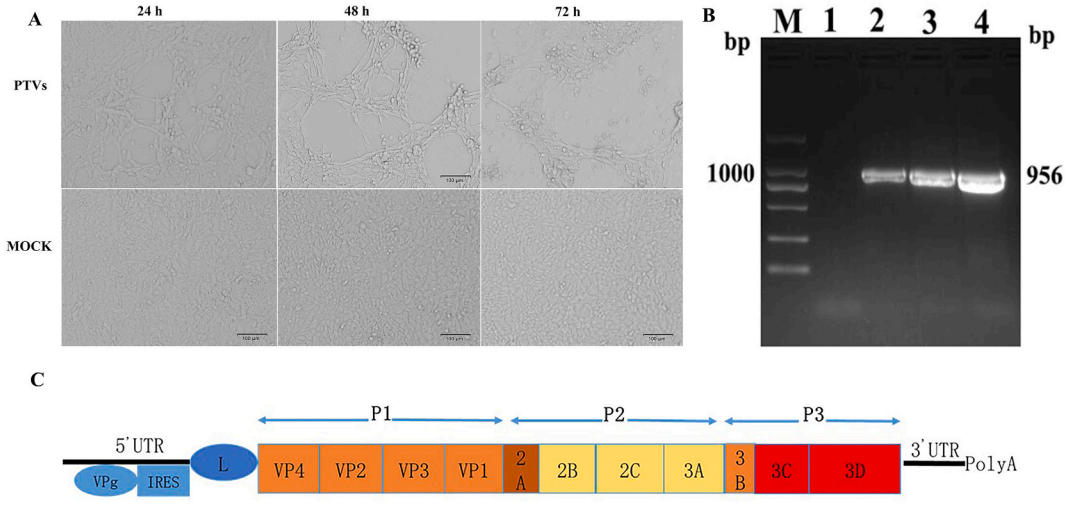

Fig. 1. Characterization of PTVs infection in ST cells. A. Morphological changes in ST cells at different time points after PTVs JS2021 infection. B. RT-PCR electrophoresis map of VP1 gene fragment of PTVs JS2021 isolate. C. The schematic diagram of genome structure of PTVs.

3.2. PTVs genome-wide structure

The total length of the genome is about 7221 bp, and the sequence of genomes is 5′UTR-L-VP4-VP2-VP3-VP1-2A-2B–2C-3A-3B–3C-3D-3′UTR (Fig. 1C). There is an un translated region (UTR) at both the 5 ‘and 3′ ends, consisting of 415 bp and 95 bp respectively, the length of the 5′-UTR is much longer than that of the 3′-UTR. Among them, 5′-UTR contains Poly (C) structure and has a small molecular weight connexin VPg, while 3′-UTR contains Poly (A) structure. The whole genome contains a large open reading frame, which is processed by protease to form P1, P2 and P3 polypeptide precursors, among which P1 is the precursor of capsid protein, and after processing, it is the capsid protein of PTV. Both P2 and P3 are precursors of nonstructural proteins, which form some intermediate precursors after maturation. These products are very stable and participate in various life activities of virus replication.

3.3. PTVs genome-wide evolution analysis

The genetic tree of PTVs JS2021 was constructed by MEGA7.0 with 50 reference sequences selected from GenBank. The result is shown in Fig. 2, PTVs JS2021 and PTV-HNMY are in the same branch and have the closest relationship (Fig. 2A), and the homology of nucleotide sequence in the whole genome range from 93.33% to 81.5% (Supplementary T. 1).

According to the phylogenetic tree of VP1 protein, PTVs JS2021 and PTV-AF 296102.1are in the same branch (Fig. 2B). The nucleotide homology of VP1 gene of PTV JS2021 with PTV-AF 296102.1 reached 82.97% (Table 2). Revealing that the VP1 protein is located in the same branch as the PTV-1 subtype. The similarity of nucleotide sequence with most sera of PTV-1 subtype was more than 80%. However, the nucleotide similarity with other serotypes is low, ranging from 60% to 80% (Supplementary T. 2).

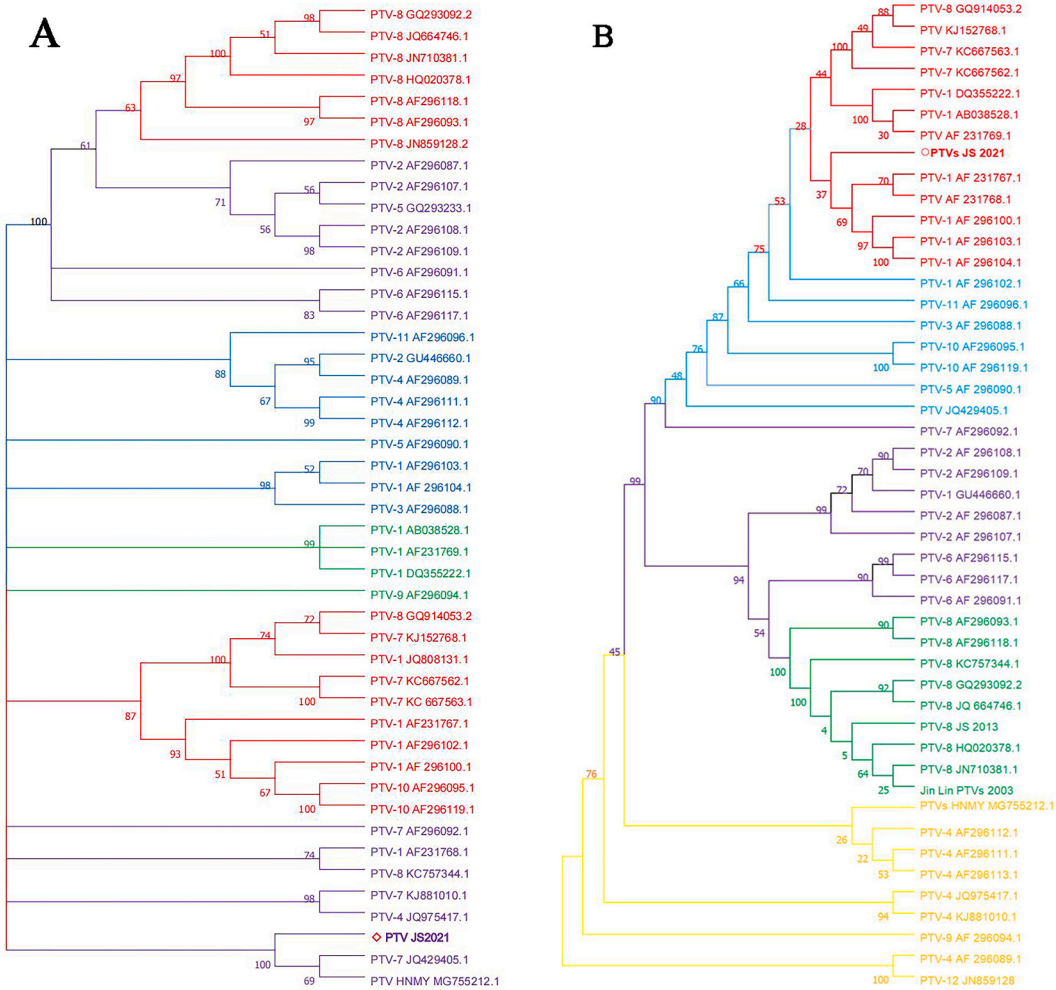

Fig. 2. (A) Neighbor-joining unrooted phylogenetic trees based on the nucleotide sequences of the full-length sequences of PTVs JS2021 and different genogroups. Our strain, PTVs JS 2021, is marked with a red triangle (◇). (B) Neighborjoining unrooted phylogenetic trees based on the VP1 gene sequences of PTVs. PTVs JS 2021, is marked with a red circle (O).

3.4. Physicochemical properties of PTVs capsid protein

Structural proteins 1A (VP4), 1B (VP2), 1C (VP3) and 1D (VP1) of PTVS constitute the capsid protein of virus particles. The VP1 is the main protective antigen, which is located on the surface of virus particles. In this study, the physical and chemical properties of VP1 of PTVs were analyzed by Port-Param online software. The result is shown in Table 1, the VP1 encodes 263 amino acids, of which 34 were serine, accounting for 12.9%, with 21 negative charges (Asp + Glu) and 22 positive charges (Arg + Lys), and has a molecular weight of 29 kDa and a theoretical isoelectric point of 7.80. Genomic fat index was 76.73, and total average hydrophilicity (GRAVY) was −0.119. The predicted half-life in mammalian reticulocytes is 30 h *in vitro*, and the half-life in *Escherichia coli* and yeast is more than 20 h and 10 h respectively. The instability index is 56.65, which indicates that the protein belongs to unstable protein.

3.5. Hydrophilicity and hydrophobicity of PTVs capsid protein

The analysis of physicochemical properties of VP1 capsid protein, showed that the GRAVY value was −0.119, which was negative, indicating that VP1 capsid protein may be hydrophilic protein. Verify the display through Protscale software, the result is shown in Fig. 3, In the PTVs-JS2021 of VP1 capsid protein (Fig. 3A), the highest score of Val (V) at position 213 was1.778, and the lowest score of Gln (Q) at position191 was −2.556. In the PTV-1 AF 296102.1 of VP1 capsid protein (Fig. 3B), the highest score of Val (V) at position 92 and the Gly (G) at position 199 was1.667, and the lowest score of Glu (E) at position 247 was-3.389, In the PTVs- HNMY of VP1 capsid protein (Fig. 3C), the highest score of Ile (I) at position 92 was 1.967, and the lowest score of Gln (Q) at position 190 was −2.566, In the PTV-8 JS 2013 of VP1 capsid protein (Fig. 3D), the highest score of Val (V) at position 217 was1.789, and the lowest score of Ser (S) at position 238 was −2.622. The hydrophilic amino acids of the capsid protein are more than the hydrophobic amino acids, so them capsid protein is indeed hydrophilic.

3.6. Prediction of PTVs capsid protein signal peptides

The signal peptide of VP1 was predicted by SignalP 5.0 Server online software. As shown in Fig. 4, SP value is signal peptide value, with an average of 0.0018, almost 0, suggesting that capsid protein does not have signal peptide and does not belong to secretory protein.

3.7. Prediction of transmembrane domain of VP1 protein of PTVs

In this study, TMHMM Server online software was used to predict the transmembrane domain of capsid protein. As shown in Fig. 5, the probability of amino acid residues in each part of the helix has no peak, indicating that capsid protein may have no transmembrane structure, and the protein is an intracellular protein.

3.8. Prediction of phosphorylation site specific to VP1 protein kinase in PTVs

In this study, the specific phosphorylation sites of capsid protein kinase were predicted in NetPhos 3.1 Server. As shown in Fig. 6, In the PTVs-JS2021 (Fig. 6A), the number of amino acids Ser (S), Thr (T) and Tyr (Y) with scores greater than 0.5 was 27, 10 and 4, respectively, which indicated that there were 41 potential phosphorylation sites of capsid protein amino acids. In the PTV-1 AF 296102.1 of VP1 protein kinase (Fig. 6B), the number of amino acids Ser (S), Thr (T) and Tyr (Y) with scores greater than 0.5 was 27, 11 and 5, respectively, which indicated that there were 43 potential phosphorylation sites of capsid protein amino acids. In the PTVs-HNMY of VP1 protein kinase (Fig. 6C), the number of amino acids Ser (S), Thr (T) and Tyr (Y) with scores greater than 0.5 was 22, 12 and 4, respectively, which indicated that there were 38 potential phosphorylation sites of capsid protein amino acids. In the PTV-8 JS2013 of VP1 protein kinase (Fig. 6D), the number of amino acids Ser (S), Thr (T) and Tyr (Y) with scores greater than 0.5 was 23, 15 and 3, respectively, which indicated that there were 41 potential phosphorylation sites of capsid protein amino acids.

3.9. Prediction of B cell linear epitope of VP1 protein of PTVs

The IEDB analysis software was used to predict the B cell linear epitope of VP1 protein. The results are shown in Fig. 7. In the PTV-JS 2021 (Fig. 7A), The highest prediction score is 2.200, the lowest score is −0.005, and the average score is 0.517. It was predicted that VP1 protein contained 10 linear epitopes. In the PTV-1 AF 296102.1 (Fig. 7B), The highest prediction score is 2.200, the lowest

Table 1
Amino acid content of VP1 protein of PTVs JS2021.

Amino acid	A	R	N	D	C	Q	E	G	H	I
Quantity	17	13	10	13	5	8	8	16	4	13
Percentage	6.5%	4.9%	3.8%	4.9%	1.9%	3.0%	3.0%	6.1%	1.5%	4.9%
Amino acid	L	K	M	F	P	S	T	W	Y	V
Quantity	21	9	8	13	23	34	18	4	8	18
Percentage	8.0%	3.4%	3.0%	4.9%	8.7%	12.9%	6.8%	1.5%	3.0%	6.8%

Table 2
Spatial structure of VP1 protein.

Struce	Alpha helia	3_{10} helix	Pi helix	Beta bridge	Extend strand
Quantity	55	0	0	0	43
Percentage	20.91%	0.00%	0.00%	0.00%	16.35%
Struce	Beta turn	Bend region	Random coil	Ambiguous states	Other states
Quantity	4	0	161	0	0
Percentage	1.52%	0.00%	61.22%	0.00%	0.00%

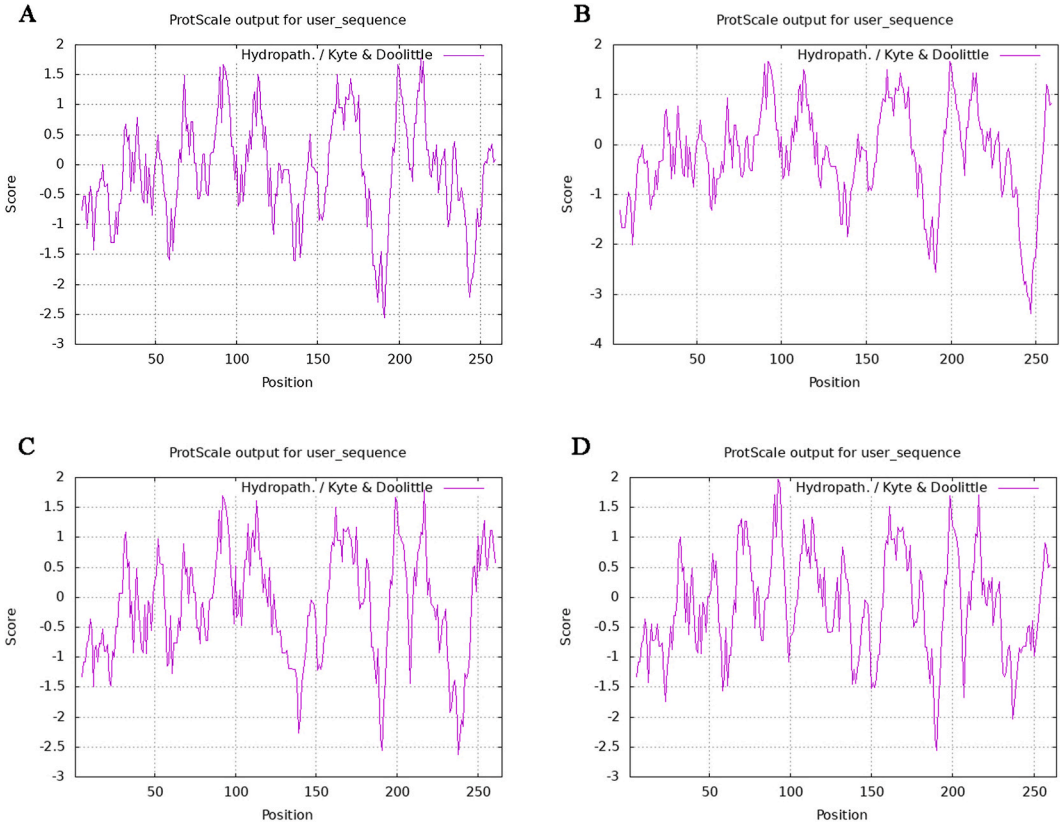

Fig. 3. Hydrophilic and hydrophobic analysis of VP1 protein. Verified by Protscale software. The peak value in the figure represents the hydrophilicity and hydrophobicity of amino acids, the highest score of Val (V) at position 213 was1.778, and the lowest score of Gln (Q) at position191 was −2.556. Figure A represents PTV JS2021. Figure B represents PTV-1 AF296102.1. Figure C represents PTV HNMY. Figure D represents PTV-8 JS2013.

score is −0.005, and the average score is 0.517. It was predicted that VP1 protein contained12 linear epitopes. It was predicted that VP1 protein contained 12 linear epitopes. In the PTVs- HNMY (Fig. 7C), The highest prediction score is 2.146, the lowest score is −0.006, and the average score is 0.212. It was predicted that VP1 protein contained 12 linear epitopes. In the PTV-JS 2013 (Fig. 7D), The highest prediction score is 2.200, the lowest score is −0.005, and the average score is 0.517.

3.10. Prediction of secondary and tertiary structure of VP1 protein of PTVs

The secondary structure of capsid protein predicted by SOPMA online software is shown in Fig. 8 (Fig. 8A), The results show that there are four other structures of capsid protein, namely irregular curl (c), extended chain (e), α-helix (h) and β-folded (t) (Fig. 8B), among which 61.22% of the structures are irregular curl, 20.91% are α-helix, 16.35% are extended chain and 1.52% are β-folded (Table 2). The SWISS-MODEL online tool is used to model the homology of capsid protein in ExPASY website. The results are shown in Fig. 9. The prediction of tertiary structure of VP1 proteinre is shown in Fig. 9 (Fig. 9A),Compared with the classical strain PTV-8jinlin/2003, The amino acid at position 129 of VP1 protein of PTVs JS2021 was mutated, which led to the reduction of alpha helix in PTVs JS2021 (Fig. 9B), This may be the cause of diarrhea in piglets.

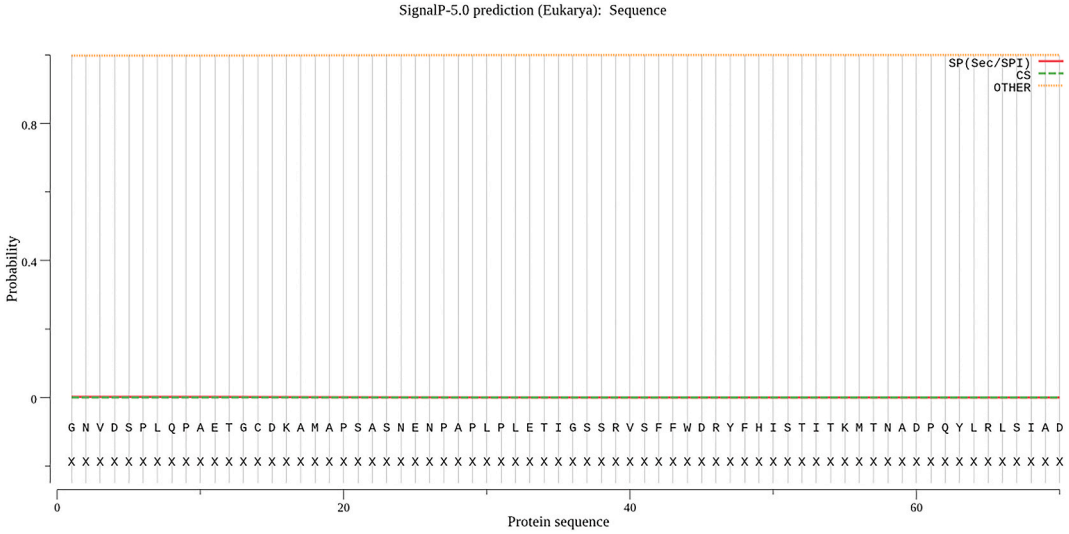

Fig. 4. Prediction of signal peptide of VP1 protein. SP is used to distinguish whether the corresponding position is a signal peptide region. CS is used to distinguish whether it is a shear site or not, and the highest peak value is the first amino acid after the shear site (i.e., the first amino acid residue of mature protein), By software analysis, there is no fluctuation in sp value, so there is no signal peptide in the protein.

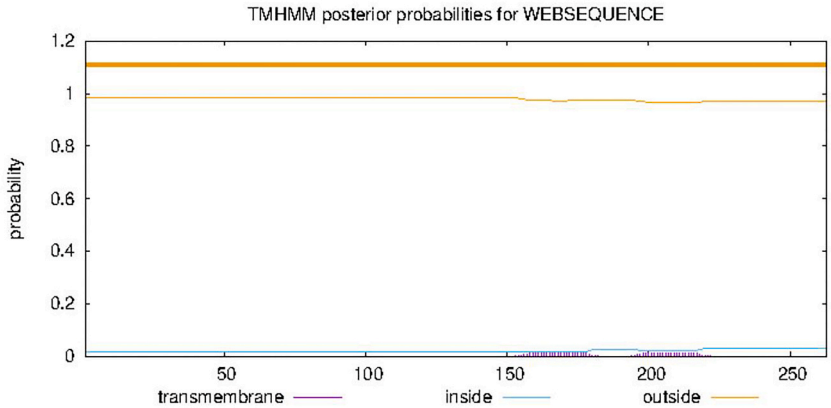

Fig. 5. Prediction of transmembrane domain of VP1 protein. The abscissa axis represents the serial number of amino acid residues corresponding to the submitted protein sequence. The value of ordinate axis is the probability value of each amino acid located in the medial membrane, lateral membrane and spiral region of crotch membrane on the transverse axis.

4. Discussion

PTVs is a causative agent of reproductive disorders [13], encephalomyelitis, respiratory diseases [14], and diarrhea in swine, with a worldwide distribution. PTVs is still frequently isolated from tonsils and other non-neural organs of apparently unaffected pigs [15]. To data, the prevalence and pathogenicity of PTVs strains has been widely reported, whereas few study focus on analysis on the complete genome of Teschovirus with swine diarrhea.

In this study, high-throughput sequencing was carried out on the feces of diarrhea piglets. A 7221bp PTVs genome was obtained, named JS2021, phylogenetic evolution analysis showed that the PTVs JS2021 strain had the closest relationship with a PTV-HNMY (MG755212.1), with a nucleotide homology of 83.74% and certain variability, The nucleotide homology of VP1 gene of PTV JS2021 with PTV-AF 296102.1 reached 82.97%, belonging to a branch of PTV-1 serotype. The nucleotide sequence with PTV-1 subtype is about 80%, Compared with other serotypes, the homology of VP1 nucleotide of PTV JS2021 was lower, almost below 80%. Suggesting that attention should be paid to the gene mutation and recombination of PTVs strain in further epidemiological investigation. It is reported that the amino acid number of VP1 protein in different serotypes of PTVs may be different, and the variation of VP1 amino acid is the main reason for the different virulence of different serotypes of PTVs strains [16]. VP1, VP2 and VP3 proteins are on the surface of virus particles, among which VP1 can not only maintain the complete morphology of virus particles, but also be the main component that determines the antigenicity of virus, and plays an important role in the binding of virus particles to receptors and virus shelling [17]. Therefore, it is of great significance to analyze the pathogenicity of vp1 protein in animals. In this

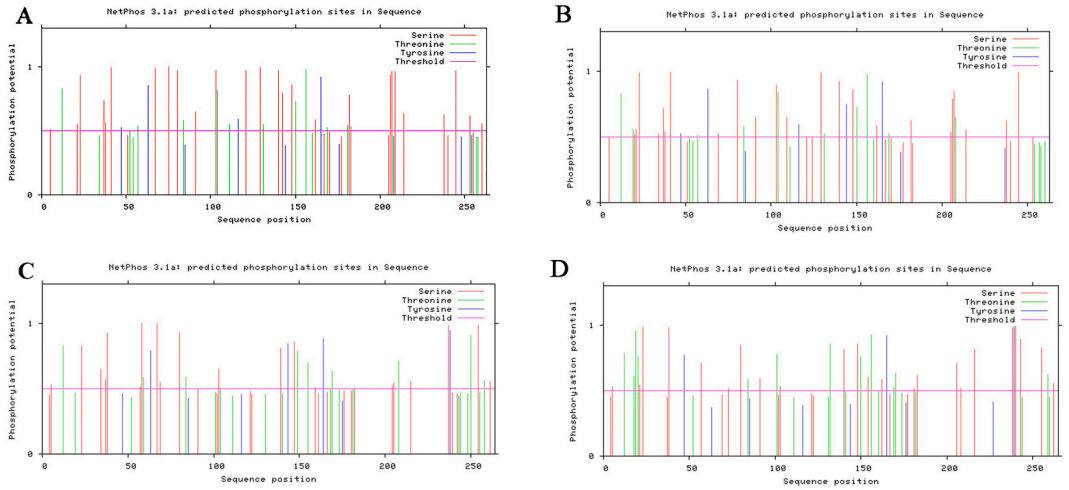

Fig. 6. Prediction of phosphorylation site specific to VP1 protein. The abscissa axis represents the serial number of amino acid residues corresponding to the submitted protein sequence. The value of ordinate axis is the score (0–1), and generally higher than 0.5 is the positive result. Figure A represents PTV JS2021. Figure B represents PTV-1 AF296102.1. Figure C represents PTV HNMY. Figure D represents PTV-8 JS2013.

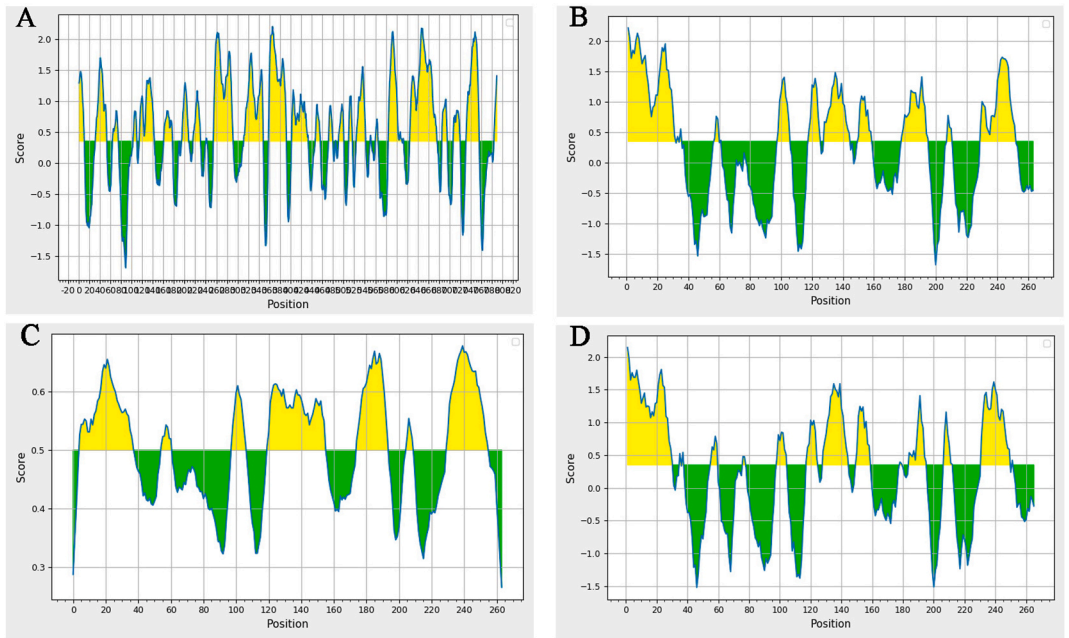

Fig. 7. Prediction of B cell linear epitope of VP1 protein. The highest score was 2.200, the lowest was-0.005, and there were 12 linear epitopes by using IEDB software. Figure A represents PTV JS2021. Figure B represents PTV-1 AF296102.1. Figure C represents PTV HNMY. Figure D represents PTV-8 JS2013.

study, the VP1 protein of PTVs was predicted and analyzed by bioinformatics technology. The results showed that the VP1 protein had a molecular weight of 29 kDa, a theoretical isoelectric point of 6.73, no transmembrane domain and no signal peptide, and was a stable hydrophilic intracellular protein with potential phosphorylation. The secondary structure prediction of capsid protein showed that there were four structures: irregular curl (c), extension chain (e), α-helix (h) and β-folded (t), among which 61.22% were irregular curls. Further prediction of protein tertiary structure showed that the tertiary structure was a heart shape, Compared with the classical strain PTV-8jinlin/2003, The amino acid at position 129 of VP1 protein of PTVs JS2021 was mutated, which led to the reduction of alpha helix in PTV JS2021, The alpha helix is an important secondary structural unit. The secondary structural units interact to form a supersecondary structure and interact to form a domain with certain functions. The domain is considered to be the smallest spatial structure unit with some functions, which can be regarded as the most basic functional entity. When the 129 th amino acid mutates on the VP1 protein of PTVs JS2021, the alpha helix decrease of PTVJS2021 may lead to changes in the tertiary structure composed of

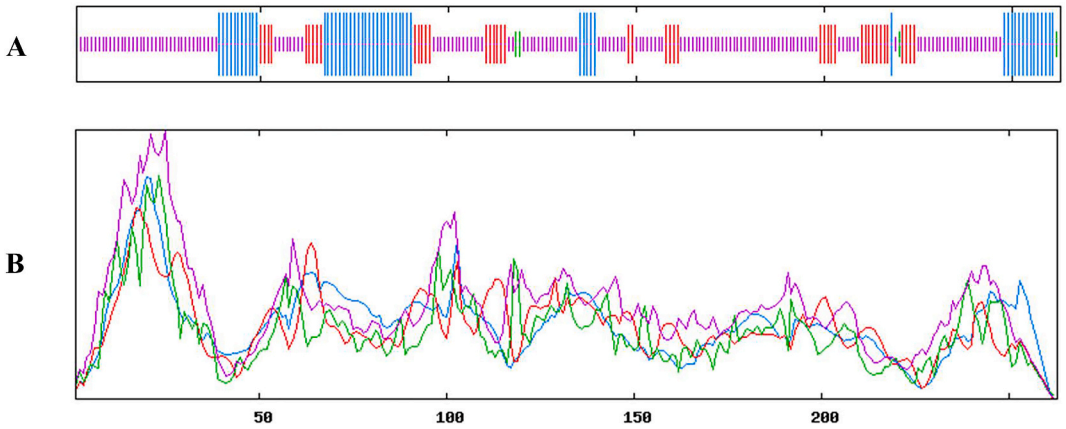

Fig. 8. Prediction of secondary structure of VP1 protein. Blue stands for Alpha helix, green stands for Beta turn, yellow stands for Random coil, and red stands for extended strand.

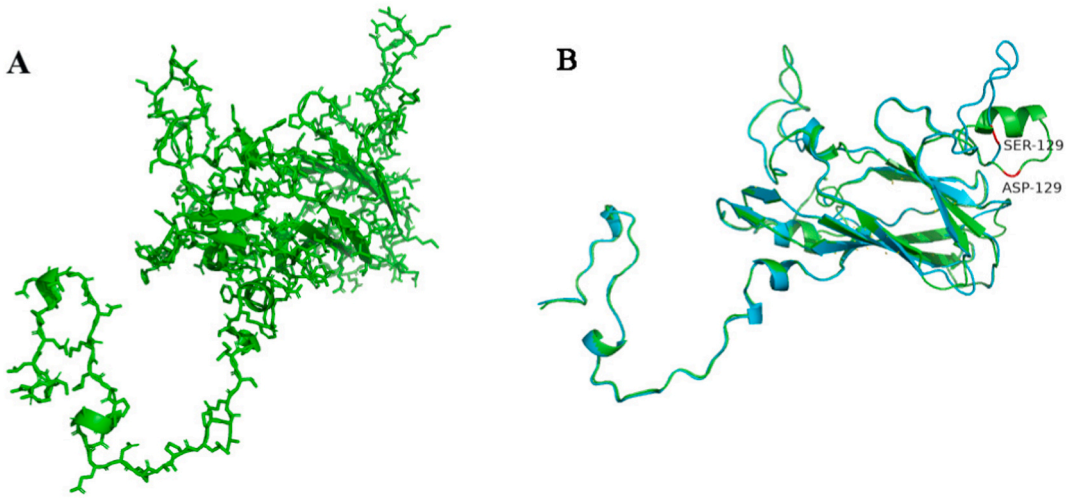

Fig. 9. Prediction of tertiary structure of VP1 protein. (A) Three-dimensional structure of VP1 protein after modeling. (B, C) Comparison of VP1 protein of PTV JS2021 with VP1 protein of classic strain PTV-8jinlin/2003, in which red represents amino acid at position 129. Among them, green stands for PTV JS 2021. Light blue represents PTV-8jinlin/2003.

single or multi-domains and change the function of proteins. This may be the cause of diarrhea in piglets. Therefore, the VP1 protein sequence of PTVs provided in this study can enrich the PTVs protein structure database, and lay a foundation for speculating the functional sites of capsid protein and predicting the structure and function in the future. In addition, it is predicted that there are multiple B cell epitopes in the protein, which may be related to the irregular curl and α-helix of the protein. The contact area of the tertiary structure is large, which is conducive to binding with the epitope, suggesting that capsid protein can be used as a good vaccine antigen, providing theoretical basis for the next development of related vaccines for disease prevention and control.

In summary, based on the bioinformatics analysis results of VP1 protein of PTVs, the genetic evolution of PTVs JS 2021 further enriched the epidemiological data of PTVs and provided powerful data for the prevention and control of PTVs. VP1 protein can be used as an effective target for developing vaccines and drugs, which is of great significance for the prevention and treatment of PTVs.

Author contribution statement

Baotai Zhang and Rongli Guo: Conceived and designed the experiments; Wrote the paper.
Baochao Fan: Performed the experiments.
Xuejiao Zhu, Jinzhu Zhou, Tao Xue and Chuanmin Liu: Analyzed and interpreted the data.
Chunyan Zhong, Xuesong Yuan, Jin Huang and Li Xiao: Contributed reagents, materials, analysis tools or data.
Xing Zhu, Jizong Li and Bin Li: Contributed reagents, materials, analysis tools and data; Wrote the paper.

Funding statement

Bin Li was supported by National Natural Science Foundation of China [32272996].

Dr Jizong Li was supported by National Natural Science Foundation of China [32002283].

This work was supported by National Key Research and Development Program (2022YFD1800601), Jiangsu province Natural Sciences Foundation (BK20221432, BK20210158), Jiangsu Agricultural Science and Technology Innovation Fund (CX (20)3094), National Natural Science Foundation of China (32272996, 32002283), Innovation Foundation of Jiangsu Academy of Agricultural Sciences (ZX(21)1217), Natural Science Foundation of Shandong Province, China (ZR2020MC019). China Postdoctoral Science Foundation (Grant No. 2022M711398 and 2022M711399), the Special Project of Northern Jiangsu (SZ-LYG202109), the "JBGS" Project of Seed Industry Revitalization in Jiangsu Province (JBGS[2021]024), Open Fund of Shaoxing Academy of Biomedicine of Zhejiang Sci-Tech University (SXAB202215), Open Fund of Key Laboratory for prevention and control of Avian Influenza and Other Major Poultry Diseases, Ministry of Agriculture and Rural Affairs, P.R. China and Key Laboratory of Livestock Disease Prevention of Guangdong Province (YDWS202213).

Data availability statement

Data included in article/supplementary material/referenced in article.

Declaration of interest statement

The authors declare that they have no known competing financial interests or personal relationships that could have appeared to influence the work reported in this paper.

Appendix A. Supplementary data

Supplementary data related to this article can be found at https://doi.org/10.1016/j.heliyon.2023.e14710.

References

[1] M. Arnold, A. Crienen, H. Swam, S.V. Berg, R. Jolie, H. Nathues, Correlation of Lawsonia intracellularis positivity in quantitative PCR and herd factors in European pig herds, Porcine Health Manag 7 (1) (2021) 13.
[2] A.S. Cornelison, L.A. Karriker, N.H. Williams, B.J. Haberl, K.J. Stalder, L.L. Schulz, J.F. Patience, Impact of health challenges on pig growth performance, carcass characteristics, and net returns under commercial conditions, Transl Anim Sci 2 (1) (2018) 50–61.
[3] M. Yamada, Y. Kaku, K. Nakamura, M. Yoshii, Y. Yamamoto, A. Miyazaki, H. Tsunemitsu, M. Narita, Immunohistochemical detection of porcine teschovirus antigen in the formalin-fixed paraffin-embedded specimens from pigs experimentally infected with porcine teschovirus, J. Vet. Med. 54 (10) (2007) 571–574.
[4] L.K. Van Breda, O.P. Dhungyel, A.N. Ginn, J.R. Iredell, M.P. Ward, Pre- and post-weaning scours in southeastern Australia: a survey of 22 commercial pig herds and characterisation of Escherichia coli isolates, PLoS One 12 (3) (2017), e0172528.
[5] K.V. Waal, J. Deen, Global trends in infectious diseases of swine, P. Natl. Acad. Sci. USA. 115 (2018) 11495–11500.
[6] T. Yang, X. Yu, B. Luo, M. Yan, R. Li, T. Qu, X. 'Ren, Epidemiology and molecular characterization of porcine teschovirus in hunan, China,transbound, Emerg. Dis. 65 (2018) 480–490.
[7] C. Zhang, S. Cui, S. Hu, Z. Zhang, Q. Guo, R. Zell, Isolation and characterization of the first Chinese strain of porcine Teschovirus-8, J. Virol. Methods. 167 (2) (2010) 208–213.
[8] M.Y. Deng, M. Millien, R. Jacques-Simon, J.K. Flanagan, A.J. Bracht, C. Carrillo, R.W. Barrette, A. Fabian, F. Mohamed, K. Moran, J. Rowland, S.L. Swenson, M. Jenkins-Moore, L. Koster, B.V. Thomsen, G. Mayr, D. Pyburn, P. Morales, J. Shaw, T. Burrage, W. White, M.T. McIntosh, S. Metwally, Diagnosis of porcine teschovirus encephalomyelitis in the republic of Haiti, J. Vet. Diagn. Invest. 24 (4) (2012) 671–678.
[9] L. Feng, H.Y. Shi, S.W. Liu, B.P. Wu, J.F. Chen, D.B. Sun, Y.E. Tong, M.S. Fu, Y.F. Wang, G.Z. Tong, Isolation and molecular characterization of a porcine teschovirus 1 isolate from China, Acta Virol 51 (2007) 7–11.
[10] T. Doerksen, T. Christensen, A. Lu, L. Noll, J.F. Bai, J. Henningson, R. Palinski, Assessment of porcine Rotavirus-associated virome variations in pigs with enteric disease, Vet. Microbiol. 270 (2022), 109447.
[11] W. Lin, S. Cui, R. Zell, Phylogeny and evolution of porcine teschovirus 8 isolated from pigs in China with reproductive failure, Arch. Virol. 157 (7) (2012) 1387–1391.
[12] R. Guo, L. Bin, L. Wen, B. Fan, K. He, Isolation and identification of Porcine teschovirus and sequencing analysis of its VP1 gene, Chin. J. Vet. Med. 53 (3) (2017) 43–46.
[13] P. Daszak, A.A. Cunningham, A.D. Hyatt, Emerging infectious diseases of wildlife-threats to biodiversity and human health, Science 287 (5452) (2000) 443–449.
[14] C. Guinat, A. Gogin, S. Blome, G. Keil, R. Pollin, D.U. Pfeiffer, L. Dixon, Transmission routes of African swine fever virus to domestic pigs: current knowledge and future research directions, Vet. Rec. 178 (11) (2016) 262–267.
[15] G. La Rosa, M. Muscillo, A.D. Grazia, S. Fontana, M. Iaconelli, M. Tollis, Validation of RT-PCR assays for molecular characterization of porcine teschoviruses and enteroviruses, J. Vet. Med. 53 (6) (2006) 257–265.
[16] M. Oba, Y.K. Naoi, M. Ito, T. Masuda, Y. Katayama, S. Sakaguchi, T. Omatsu, T. Furuya, H. Yamasato, F. Sunaga, S. Makino, T. Mizutani, M. Nagai, Metagenomic identification and sequence analysis of a Teschovirus A-related virus in porcine feces in Japan, 2014-2016, Infect. Genet. Evol. 66 (2018) 210–216.
[17] T. Tsai, C. Chang, F. Wang, A highly conserved epitope (RNNQIPQDF) of porcine teschovirus induced a group-specific antiserum: a bioinformatics-predicted model with pan-PTV potential, Viruses 12 (11) (2020) 1225.